A shift from phenol to silica-based leaf defenses during long-term soil and ecosystem development

A shift from phenol to silica-based leaf defenses during long-term soil and ecosystem development

Felix de Tombeur[1*], Etienne Laliberté[2,3], Hans Lambers[3], Michel-Pierre Faucon[4], Graham Zemunik[3], Benjamin L. Turner[5], Jean-Thomas Cornelis[1], Grégory Mahy[1]

[1]TERRA Teaching and Research Centre, Gembloux Agro-Bio Tech, University of Liege, Gembloux, Belgium.

[2]Institut de Recherche en Biologie Végétale, Université de Montréal, 4101 Sherbrooke Est, Montréal, QC H1X 2B2, Canada.

[3]School of Biological Sciences, The University of Western Australia, Crawley (Perth), WA 6009, Australia.

[4]AGHYLE, SFR Condorcet FR CNRS 3417, UniLaSalle, 19 rue Pierre Waguet, 60026, Beauvais, France.

[5]Smithsonian Tropical Research Institute, Apartado 0843-03092, Balboa, Ancon, Panama.

*Corresponding author ; 27 Avenue Maréchal Juin Bâtiment 52 – 5030 Gembloux (Belgium) ; +32488273660 ; felix.detombeur@uliege.be

Statement of authorship: All the authors conceived the ideas and designed methodology; FdT and GZ collected the samples; FdT analyzed the data and led the writing of the manuscript. All authors contributed critically to the drafts and gave final approval for publication.

Data accessibility statement: The data are available via the Dryad Digital Repository (add the link here)

Article type: Letters/Ideas & Perspectives

Running title: Leaf defenses during ecosystem development

Keywords: plant defense strategies ; silica-based defense ; plant silicon ; plant phenols ; resource availability hypothesis ; soil fertility gradient ; plant-herbivore interactions ; phenylalanine; resource limitation ; tradeoffs

Number of words in the Abstract (148), in the Main Text (5000)

Number of References: 99 (+ 3 references in the Supplementary Information)

Number of Figures and Tables: 6

Abstract

The resource availability hypothesis predicts that plants adapted to infertile soils have high levels of anti-herbivore leaf defenses. This hypothesis has been mostly explored for secondary metabolites such as phenolics, while it remains underexplored for silica-based defenses. We determined leaf concentrations of total phenols and silicon (Si) in plants growing along the 2-million-year Jurien Bay chronosequence, exhibiting an extreme gradient of soil fertility. We found that nitrogen (N) limitation on young soils led to a greater expression of phenol-based defenses, whereas old, phosphorus (P)-impoverished soils favored silica-based defenses. Both defense types were negatively correlated at the community and individual species level. Our results suggest a tradeoff among these two leaf defense strategies based on the strength and type of nutrient limitation, thereby opening up new perspectives for the resource availability hypothesis and plant defense research. This study also highlights the importance of silica-based defenses under low P supply.

Introduction

38 The resource availability hypothesis (RAH) (Coley *et al.* 1985) predicts that plant species adapted

39 to resource-rich environments will have rapid growth rates and leaf turnover, high leaf nutrient

40 concentrations, but low levels of anti-herbivore defenses. By contrast, the benefits of allocating

41 resources to anti-herbivore defenses become advantageous for species adapted to nutrient-poor

42 environments, because biomass loss by herbivory represents a significant loss of scarce nutrients

43 (Coley *et al.* 1985; Endara & Coley 2011). This theory has been primarily explored with regard to

44 secondary metabolites (e.g. phenolics), plant mechanical properties and nitrogen (N)-based

45 defenses, while silica-based defenses have received far less attention (Endara & Coley 2011). For

46 instance, in a meta-analysis testing the global consistency of the RAH (Endara & Coley 2011), the

47 deposits of silica bodies in plants as defense mechanism (McNaughton *et al.* 1985; Hartley &

48 DeGabriel 2016) represented only 1% of statistical tests considered in the literature (Massey *et al.*

49 2007). This highlights the fact that Si-based defenses have been understudied by plant ecologists,

50 despite representing one of the earliest anti-herbivore plant adaptations (Trembath-Reichert *et al.*

51 2015; Deshmukh *et al.* 2020).

52 Vascular plants can accumulate silicon (Si) in concentrations exceeding those of the major nutrients

53 (0.1 to 10% of dry weight; Epstein 1994). Taken up as monosilicic acid (H_4SiO_4) from the soil

54 solution, Si is translocated to sites of rapid transpiration, where it polymerizes as amorphous

55 hydrated silica ($SiO_2.nH_2O$) between cell walls and the lumen, and in extracellular and intercellular

56 spaces of the leaf epidermis (Kumar *et al.* 2017; de Tombeur *et al.* 2020a). This mechanism of

57 biosilicification has occurred in land plants for over 400 million years (Trembath-Reichert *et al.*

58 2015) and provides numerous benefits to plants, including resistance to abiotic stresses such as

59 metal toxicity, salinity, nutrient deficiency or water stress (Cooke & Leishman 2016; Debona *et al.*

60   2017; Frew *et al.* 2018). Biosilicification also reduces herbivory by increasing leaf abrasiveness,

61   which reduces penetration and chewing, and by decreasing the digestibility and palatability of

62   leaves (Massey & Hartley 2006, 2009; Massey *et al.* 2006, 2007; Johnson *et al.* 2020). Besides

63   physical defenses, biosilicification has been linked to anti-herbivore phytohormonal signaling

64   through the modulation of jasmonic acid, salicylic acid and ethylene, resulting in modified

65   emissions of volatile organic compounds (Coskun *et al.* 2019; Leroy *et al.* 2019). Although the

66   impact of silica-based defenses on herbivory has mainly been studied in Poales (e.g., grasses), it is

67   now well-established that the positive role of Si in biotic stresses is not restricted to Si-

68   accumulating families (Fauteux *et al.* 2006; Deshmukh *et al.* 2013; Katz 2014; Johnson *et al.* 2019;

69   Putra *et al.* 2020). Other taxa can have [Si] as high as in grasses (Hodson *et al.* 2005; Katz 2014),

70   Si transporters have been identified in some legume species (Deshmukh *et al.* 2013), and it has

71   recently been demonstrated that Si is an effective defense against herbivory in soybean (Fabaceae),

72   even at moderate leaf [Si] (Johnson *et al.* 2019). Despite these evidences, the expression of Si-

73   based defenses along soil fertility gradients remains underexplored, although we might expect them

74   to increase with declining soil fertility as predicted by the RAH.

75   Besides silica-based defenses, one of the most important classes of plant defenses are phenolics

76   compounds, which have been shown to co-vary with silica-based defenses (Cooke & Leishman

77   2012). In accordance with the RAH, high levels of phenolic compounds have long been considered

78   as having adaptive value for plants growing on infertile soils (Bryant *et al.* 1983; Coley *et al.* 1985;

79   Northup *et al.* 1995; Hättenschwiller *et al.* 2003; Kraus *et al.* 2004). It has been proposed that N

80   limitation leads to a greater expression of phenol-based defenses than phosphorus (P) limitation,

81   because N limitation impacts the phenylpropanoid pathway more strongly, which is involved in

82   the synthesis of both aromatic amino acids and phenol compounds (Haukioja *et al.* 1998; Jones &

83   Hartley 1999; Wright *et al.* 2010). While this hypothesis received support in some studies (Wright

84   *et al.* 2010; de Long *et al.* 2016), others have instead found that P limitation significantly increases

85   plant phenol synthesis (Hättenschwiller *et al.* 2003; Sampedro *et al.* 2011; Zhang *et al.* 2012).

86   However, these studies generally considered one single species and/or performed fertilization to

87   simulate nutrient limitations, while community-level studies in natural environments have not been

88   conducted. Strong natural shifts from N to P limitation of plant productivity that occur during long-

89   term soil and ecosystem development (Vitousek *et al.* 1993; Laliberté *et al.* 2012) might therefore

90   impact plant phenol synthesis differently in species-rich plant communities, but this has not been

91   explored. Furthermore, the potential covariation of phenolic foliar defenses with silica-based ones

92   (Cooke & Leishman 2012) has never been studied along soil fertility gradients.

93   We determined leaf Si and total phenol concentrations in plants growing along the 2 million-year

94   Jurien Bay soil chronosequence in south-western Australia (Turner & Laliberté 2015). This long-

95   term soil chronosequence comprises a series of coastal dunes within a global biodiversity hotspot,

96   supporting species-rich shrubland under a Mediterranean climate (Zemunik *et al.* 2016). It exhibits

97   an extreme gradient of soil fertility in terms of rock-derived nutrients (P, calcium, magnesium,

98   potassium), and shifts from N to P limitation of plant productivity as soils age (Laliberté *et al.*

99   2012; Hayes *et al.* 2014). Leaf concentrations of major plant nutrients decrease sharply with

100   ecosystem age (Hayes *et al.* 2014; de Tombeur *et al.* 2020c), and plants converge towards highly

101   efficient nutrient-use strategies on the oldest, most nutrient-impoverished soils (Hayes *et al.* 2014;

102   Guilherme Pereira *et al.* 2019). The youngest soils can also be considered infertile from an N

103   standpoint since their N capital has not yet built up and plant growth on these soils is limited by

104   low N availability (Laliberté *et al.* 2012; Hayes *et al.* 2014). Long-term soil chronosequences that

105   cover both the progressive and retrogressive phases of ecosystem development provide

106   exceptionally strong natural soil fertility and productivity gradients (Vitousek 2004; Peltzer *et al.*

107   2010) along which predictions of the RAH can be tested. Furthermore, the stoichiometric shifts

108   from N to P limitation of plant growth that occur along such retrogressive soil chronosequences

109   (Peltzer *et al.* 2010; Laliberté *et al.* 2012; Hayes *et al.* 2014) allow us to explore extensions of the

110   RAH about the type of foliar defenses that are expressed depending on the type of nutrient

111   limitation (e.g. N vs P on plant phenols: Wright *et al.* 2010; de Long *et al.* 2016), which have never

112   been explored.

113   In accordance with the RAH, we hypothesized a greater expression of anti-herbivore defenses in

114   plants growing on the oldest (P-limiting) and the very youngest (N-limiting) soils, compared with

115   the intermediate-aged and most fertile soils where plant productivity, N and P availability peak

116   (Laliberté *et al.* 2012, 2014), but further hypothesized that the type of defense most strongly

117   expressed would depend on the type of nutrient limitation. Specifically, we hypothesized higher

118   leaf phenol concentrations on the younger soils given the expected impact of N limitation on the

119   phenylpropanoid pathway, whereas we expected silica-based defenses to be most strongly

120   expressed in the oldest, P-impoverished soils. We expect the community-level patterns to be mostly

121   driven by changes in plant species composition since the Jurien Bay chronosequence is

122   characterized by a strong species turnover (Zemunik *et al.* 2016). This species turnover reflects the

123   expression of selective edaphic forces acting on a species-rich regional flora over an ecological

124   time scale (Laliberté *et al.* 2014).

125   **Materials and methods**

126   *Study area and site description*

5

127   The 2 Ma Jurien Bay chronosequence is located in south-western Australia, approximately 200 km

128   north of Perth (Fig. S1), and is described in detail in Laliberté *et al.* (2012) and Turner & Laliberté

129   (2015). The chronosequence, part of the Swan Coastal Plain, comprises a series of dunes parallel

130   to the coast, formed by periodic interglacial sea-level high-stands since the Early Pleistocene/Late

131   Pliocene (Kendrick *et al.* 1991), with a clear gradient of soil age with increasing distance from the

132   Indian Ocean. The dunes comprise three units: the Quindalup dunes date from the Holocene (up to

133   7 ka), the Spearwood dunes from the Middle Pleistocene (120 to 500 ka) and the Bassendean dunes

134   from the Early Pleistocene or Late Pliocene (~2 Ma) (McArthur & Bettenay 1974; Playford *et al.*

135   1976). The parent material of the dunes is calcareous sand from the nearshore coastal environment

136   (Turner & Laliberté 2015). The climate is Mediterranean, with a mean annual temperature of 19°C,

137   mean annual rainfall 533 mm and potential annual evapotranspiration of 1433 mm, which results

138   in a water balance of –900 mm yr^{-1} (data from the Jurien Bay Bureau of Meteorology from 1968

139   to 2015 in Turner *et al.* (2018).

140   We selected the same five chronosequence stages as in Hayes *et al.* (2014); these include both the

141   early and retrogressive phases of long-term ecosystem development. The main soil properties of

142   these five stages can be found in Table 1. Soil total P and carbonate concentrations, cation exchange

143   capacity and pH-$CaCl_2$ continually decrease with increasing soil age. Soil total N concentrations

144   increase from stage 1 to stage 2 during the progressive phase of ecosystem development, then

145   decrease towards the last stages during the retrogressive phase (Laliberté *et al.* 2012; Turner &

146   Laliberté 2015). Plant growth is most strongly limited by low N availability in the early stages, and

147   by P availability in the advanced stages (Laliberté *et al.* 2012; Hayes *et al.* 2014). Previous studies

148   showed that plant-available [Si] is low in the early stages of soil development, increases in stage 4

149   in the Spearwood dune system, and finally decreases in the oldest stage of soil development, where

150   it is controlled by intense biocycling (Table 1) (de Tombeur *et al.* 2020b, c).

151   *Site selection*

152   For each chronosequence stage, we randomly selected five plots (10 m × 10 m each) among the 10

153   plots already characterized for soil and vegetation in previous studies (Hayes *et al.* 2014; Zemunik

154   *et al.* 2016) (Fig. S1). The plots were originally selected using a random stratified sampling design

155   (Zemunik *et al.* 2016). To characterize vegetation, seven 2 m × 2 m subplots were randomly

156   positioned in each plot in which all individuals of all vascular plant species were counted (Zemunik

157   *et al.* 2016). The percent canopy cover of each species was estimated, and the relative cover of

158   each species was calculated as a fraction of the total canopy cover over the seven subplots

159   (Zemunik *et al.* 2016).

160   *Sampling procedure*

161   In the 25 plots selected, we sampled leaves according to two procedures. First, we sampled leaves

162   from one individual plant for each of the 10 most-abundant species of each plot as defined in

163   Zemunik *et al.* (2016). The number of leaves sampled per individual was adapted according to their

164   mass, but was never less than 10. Occasionally, a species originally included in the 10 most-

165   abundant species was not found on the plot, which resulted in less than 10 species for some plots

166   (Table S1). The 234 species sampled with this first procedure still accounted for 57% to 88% of

167   the total cover of each plot (Table S1). The community-level analyses were performed only on

168   these species. Second, we systematically sampled the species belonging to nine families, even if

169   they were not included in the 10 most-abundant species, in order to study family-level variation in

170   leaf [Si] and [phenols], following the same sampling procedure: Asparagaceae, Cyperaceae,

171 Ericaceae, Fabaceae, Haemodoraceae, Myrtaceae, Poaceae, Restionaceae and Rhamnaceae (Table

172 S2). These families were selected because they were well represented and found at all stages of the

173 chronosequence (Zemunik *et al.* 2016), and likely had contrasting [Si] based on known

174 phylogenetic patterns (Hodson *et al.* 2005). In total, 298 leaf samples belonging to 24 families were

175 collected (Tables S1 and S2).

176 All leaf material was collected over two weeks in November 2018. Leaves were sampled from one

177 healthy mature individual plant per species in each plot; when an individual did not provide

178 sufficient biomass for analysis (e.g., Poaceae spp.), leaf samples from several individuals within

179 the plot were combined.

180 *Leaf analyses*

181 Leaves were washed with distilled water, dried at 70 °C for 48 h and finely ground. Leaf material

182 (0.5 g) was placed in a porcelain crucible and calcinated at 450°C for 24 h. The weight after

183 calcination was used to calculate the ash content. The ash was mixed with 1.6 g lithium-metaborate

184 and 0.4 g of lithium-tetraborate in a graphite crucible and heated at 1000 °C for 5 min (Chao &

185 Sanzolone 1992). The bead was then dissolved in 15% HNO_3 and the concentrations of Si, P,

186 calcium (Ca), magnesium (Mg) and potassium (K) were determined by inductively coupled

187 plasma-optical emission spectrometry (Agilent Technologies, 700 series ICP-OES). Phenolic

188 compounds were extracted from a 0.25 g ground sample stirred with 10 mL of 70% acetone for 30

189 min (Salminen & Karonen 2011; Schaller *et al.* 2012; Bettaieb Rebey *et al.* 2020). Total phenols

190 were determined in triplicate as described in Salminen & Karonen (2011) using a Folin-Ciocalteu

191 assay with gallic acid monohydrate as standard (Merckx, Darmstadt, Germany). Total phenol

192 concentrations were expressed as g of gallic acid equivalents (GAE) per kilogram of dry weight.

Soil sampling and analyses

In order to determine how Si availability in soils affected species-level variations in leaf [Si], three soil samples (top 20 cm) were taken in each of the 25 plots, for a total of 75 soil samples. Samples were air-dried and sieved (< 2 mm). The pool of 'plant-available Si' was determined by extraction in 0.01 M $CaCl_2$ (Haymsom & Chapman 1975; Sauer *et al.* 2006). Soil was shaken for 5 h in a 1:10 soil-to-solution ratio, filtered (cellulose filter, pore size < 2 μm, Healthcare Whatman™), acidified with 50 μL of ultrapure 65% HNO_3, and stored in darkness at 4°C prior to Si determination by ICP-OES.

Data analyses

To characterize leaf [phenols], [Si], [Ca], [Mg], [K] and [P] in plant communities across the chronosequence, we calculated the mean values of the 10 most-abundant species per plot, weighted or not by their relative canopy cover. The cover-weighted mean (CWM) was calculated as follows (Garnier *et al.* 2004; Violle *et al.* 2007):

$$CWM = \sum_{i=1}^{S} t_i \times RC_i$$

where t_i and RC_i are, respectively, the value of the trait t and its relative cover RC for a species i and S is the number of species.

The differences in plant-available [Si], leaf [phenols], [Si], [P], [Ca], [Mg] and [K] across the chronosequence stages were tested by one-way analysis of variance (ANOVA), followed by *post-hoc* multiple comparison (Fisher's Least Significant Difference [LSD] tests). When these analyses considered all individuals together (i.e., not the mean and CWM of the plant communities), we treated species and plots as a random factor (mixed-effect models). We tested the relationships

214 between leaf [Si], [phenols] and major soil properties (total P, total N, ratio soil N:P) with linear

215 mixed-effect models, treating plot and species as random factors when all individuals were

216 considered together, and treating chronosequence stage as a random factor when the means and

217 CWM of the 25 plots were considered. We also explored relationships between leaf [Si], [phenols]

218 and foliar nutrient concentrations through Pearson tests of correlation. For the nine plant families

219 selected, we tested the differences in leaf [phenols] and [Si] across the chronosequence stages using

220 mixed-effect models with species and plot as random factors, followed by Fisher's LSD tests, and

221 we tested the relationships between leaf [Si] and [phenols] with linear mixed-effect models (with

222 plot and species as random factors). Additionally, we studied intraspecific variation for seven taxa,

223 and detailed explanation of the statistical analyses used is presented in the Supplementary

224 Information. Finally, a t-test was performed to examine the differences in leaf [Si] between dicots

225 and monocots. All residuals were visually inspected for heteroscedasticity and appropriate

226 transformations were performed to meet the model assumptions. All analyses were conducted in R

227 using the 'nlme' (Pinheiro *et al.* 2020) and 'multcomp' (Hothorn *et al.* 2008) packages.

Results

Community-level leaf concentrations of Si, total phenols and major nutrients across the chronosequence stages

231 Leaf [Si] increased with increasing soil age, whether all individuals were considered together or

232 the means and CWM of the 25 communities (Fig. 1a). The mean leaf [Si] within the 25

233 communities increased from stage 1 (0.5 ± 0.2 g kg^{-1}) to stages 2 and 3 (1.6 ± 0.4 and 2.4 ± 0.4 g

234 kg^{-1}), and then to stages 4 and 5 (3.3 ± 1.2 and 4.2 ± 1.3 g kg^{-1}). The CWM followed the same

235 pattern (Fig. 1a). The CWM leaf [Si] was negatively correlated to soil total P and positively

236 correlated to soil N to P ratio (Fig. 2a), as for the means (Fig. S2).

237   By contrast, leaf [phenols] decreased with increasing chronosequence stage, whether all individuals

238   were considered together or the means and CWM of the 25 communities (Fig. 1b). However, only

239   stages 1-2 and 5 were significantly different from each other when all individuals were considered

240   together. The mean leaf [phenols] decreased from stage 1 (48.9 ± 5.5 GAE g kg^{-1}) to stage 5 (42.6

241    $\pm$ 3.9 GAE g kg^{-1}), as did the CWM (from 51.1 ± 5.1 to 42.9 ± 3.9 GAE g kg^{-1}). The CWM leaf

242   [phenols] was positively correlated to soil total P and negatively correlated to soil N to P ratio (Fig.

243   2b), as for the means (Fig. S2).

244   Leaf [phenols] and [Si] were correlated negatively with each other when all individuals were

245   considered (Fig. 3a), with the means and CWM of each community (Fig. 3b, c), and when species

246   means were considered (Fig. S3). Leaf [ash], [Ca], [Mg], [K] and [P] decreased with increasing

247   soil age (Fig. S4). Major leaf nutrient concentrations, including P, were therefore negatively

248   correlated with leaf [Si], whether all samples were considered individually or as means and CWM

249   of the 25 communities (Fig. 3d).

250   *Family and species-level leaf concentrations of Si and total phenols across the chronosequence*

251   Within the Cyperaceae, leaf [Si] significantly increased with increasing soil age while leaf

252   [phenols] decreased, and both defense types were negatively correlated through species

253   replacement across the chronosequence (Fig. 4). In other plant families, leaf [Si] increased or was

254   constant with increasing soil age, while the opposite was found for [phenols], but a significant

255   negative relationship between both defense types was identified only for the Restionaceae (Fig.

256   S5). For the seven species for which intra-specific variation was assessed, the mixed-effect models

257   showed that leaf [Si] significantly increased with increasing chronosequence stage while the

258   opposite was found for [phenols] (Table S3).

11

259 *Impact of species replacement, intra-specific and inter-specific variation on the community-level*

260 *leaf [Si] and [phenols]*

261 Soil plant-available [Si] was lowest in stages 1 and 2 (1.5 ± 0.4 mg kg^{-1}), increased in stage 3 (4.0

262 ± 0.3 mg kg^{-1}), then in stage 4 (9.4 ± 1.0 mg kg^{-1}), before it decreased at the oldest stage (4.3 ± 0.2

263 mg kg^{-1}) (Table S4). Leaf [Si] was positively related to plant-available [Si] for three species of the

264 seven (*Lepidosperma calcicola*, *Desmocladus asper* and *Acacia lasiocarpa* var. *lasiocarpa*) for

265 which intra-specific variations were considered (Table S5). These species tended to accumulate

266 more Si than those that did not show a correlation with plant-available [Si]. Despite this relationship

267 between plant-available [Si] and leaf [Si] at the species-level (more pronounced for Si-

268 accumulating species, with the exception of *Conostylis candicans* subsp. *calcicola*), the increase

269 of the CWM leaf [Si] with increasing soil age was primarily driven by changes in the dominant

270 plant families across the chronosequence (Fig. S6). The increase of the mean and CWM leaf [Si]

271 with increasing soil age was not only driven by changes in the dominant families, but also within

272 families and genera, which is described as Supplementary Results.

273 The plant families with the strongest contribution to the CWM leaf [phenols] strongly differed

274 across the chronosequence (Fig. S6), highlighting the importance of species replacement on the

275 patterns observed at the community level. In contrast to leaf [Si], the contribution of each family

276 to the CWM [phenols] was proportional to its relative cover, highlighting less variation in [phenols]

277 among families.

Discussion

279 Overall, our results do not support the main prediction of the RAH, since investments in the two

280 anti-herbivore defenses considered were not the lowest at the most fertile soils, where both N and

281   P availability and plant productivity peak (stages 2 and 3) (Laliberté *et al.* 2012). Instead,

282   community-level leaf [Si] was highest on old, nutrient-impoverished soils, where P limits plant

283   productivity, while leaf [phenols] were the highest on young soils, where plant productivity is

284   limited by N, and both defenses were negatively correlated with each other (Fig. 5). Nevertheless,

285   only two types of chemical defense were considered in this study and the hypothesis of an overall

286   greater investment in defenses in the least fertile soils as predicted by the RAH should consider the

287   full array of anti-herbivore defenses, including structural, physical and qualitative chemical

288   defenses (Aplin & Cannon 1971; Moles *et al.* 2013; Lambers & Oliveira 2019).

289   The use of soil chronosequences allows us to minimize effects of other ecosystem properties (e.g.,

290   climate, topography, parent material, salt content) beyond soil age and associated changes in major

291   nutrients (e.g. N, P) that might influence leaf [Si] and [phenols], yet we cannot rule completely out

292   other covarying factors. In particular, soil pH declines along the chronosequence which could

293   indirectly impact plant-available [Si] (de Tombeur *et al.* 2020b). However, our previous work has

294   shown that community-level changes in foliar [Si] with soil age across this chronosequence

295   primarily arise from plant species turnover toward those that accumulate foliar [Si] as soil P

296   availability declines, and not directly because of pH-induced changes in Si availability (de

297   Tombeur *et al.* 2020c). Similarly, since soil nutrient availability has a greater impact on plant

298   phenol concentrations than soil pH (Kraus *et al.* 2004), we interpret the changes in foliar [Si]| and

299   [phenols] mainly in terms of changes in soil N and P availability that are the major drivers of plant

300   community assembly along the Jurien Bay chronosequence (Laliberté *et al.* 2014).

301   *Convergence towards silica-based defenses during ecosystem retrogression*

302   Our results show a convergence towards plants having higher leaf [Si] on P-impoverished soils,

303   during ecosystem retrogression. Indeed, despite the decrease of plant-available [Si] in the last stage,

304 induced by soil desilication (de Tombeur *et al.* 2020b), the intense cycling of highly-soluble plant-

305 derived Si in the oldest soils allows maintenance of high leaf [Si] (de Tombeur *et al.* 2020c). The

306 convergence towards plants having higher leaf [Si] with increasing nutrient depletion was

307 accompanied by a strong decrease in leaf macronutrient concentrations, including N (Hayes *et al.*

308 2014; Guilherme Pereira *et al.* 2019), and an increase in leaf mass per area (LMA) and leaf dry

309 matter content (LMDC) along the Jurien Bay chronosequence (Guilherme Pereira *et al.* 2019).

310 These traits highlight the convergence towards slow-growing plants adapted to P-impoverished

311 soils and nutrient-poor environments with increasing soil age (Lambers & Poorter 1992; Wright *et*

312 *al.* 2004; Garnier & Navas 2013; Reich 2014). Their higher leaf [Si] suggests that these species

313 have evolved towards higher levels of silica deposits to minimize biomass and nutrient loss by

314 herbivores in these nutrient-poor environments, in line with the RAH (Coley *et al.* 1985).

315 Following this hypothesis, the likely longer leaf lifespan of these species could partly explain their

316 higher expression of silica-based defenses, since Si accumulates as a leaf ages (Motomura *et al.*

317 2002).

318 An alternative but not necessarily mutually exclusive hypothesis could be mitigation of P stress.

319 The first evidence for a positive effect of Si for plants growing under P stress came from the

320 Rothamsted Experimental Station (Hall & Morison 1906). Since then, other studies have made

321 similar observations (Ma & Takahashi 1990; Neu *et al.* 2017) and Quigley *et al.* (2020) recently

322 proposed that high levels of biosilicification might be an adaptation to resource-poor environments.

323 Although the mechanisms proposed are numerous and diverse, the positive role of Si under P stress

324 is becoming clearer (Kostic *et al.* 2017), and could explain the convergence towards species having

325 higher leaf [Si] with increasing P depletion. Overall, our results suggest that leaf Si is associated

326 with the 'slow' end of the leaf economics spectrum (Wright *et al.* 2004; Reich 2014), with species

327   having long-lived leaves with low macronutrient concentrations and high LMA and LDMC, but

328   this hypothesis requires further investigation.

329   The increase of the CWM leaf [Si] from the P-limited ecosystem in stage 4 is partly explained by

330   Proteaceae having high relative cover and relatively high [Si] for dicot species (up to 6.8 g kg^{-1}

331   DW; Hodson *et al.* 2005). We have no information on Si transporters (Ma *et al.* 2006) in

332   Proteaceae, but it is possible that the exudation of carboxylates in the rhizosphere by their cluster

333   roots (Lambers *et al.* 2008) mobilizes Si from poorly-soluble minerals, thus favoring its uptake.

334   These cluster roots release carboxylates into the rhizosphere and release P from strongly sorbed

335   inorganic forms (Lambers *et al.* 2008), but also mobilize micronutrients such as manganese (Mn)

336   (Lambers *et al.* 2015; Pang *et al.* 2018). Some carboxylate-releasing roots mobilize P from rocks

337   that are highly resistant to weathering, such as quartzite (Teodoro *et al.* 2019). The relatively high

338   leaf [Si] in some dicot species exhibiting such specialized P-acquisition strategies might therefore

339   be explained by their mobilization of Si through carboxylate exudation into the rhizosphere. More

340   generally, this mechanism might explain the convergence towards leaves with higher [Si] with

341   increasing nutrient-depletion, because the relative cover of cluster-rooted species increases

342   markedly along the Jurien Bay chronosequence (Fig. 5) (Zemunik *et al.* 2015), and other species

343   might benefit from the carboxylate exudation of their neighbors (Lambers *et al.* 2018). This

344   mechanism may also explain why we observed species with some of the highest leaf [Si] found in

345   literature (up to 43 g kg^{-1} DW for *Mesomelaena pseudostygia* at stage 4) (Schoelynck *et al.* 2010;

346   Carey *et al.* 2017, 2019; Schaller *et al.* 2018; Ishizawa *et al.* 2019; Nakamura *et al.* 2019) although

347   the Jurien Bay soils are among the most desilicated worldwide, with one of the lowest Si

348   availability for plants (de Tombeur *et al.* 2020b).

349   *Nitrogen limitation and phenol synthesis on young soils*

350 The CWM leaf [phenols] slightly, but significantly, decreased with increasing soil age, which we

351 interpreted as resulting from the N-limiting conditions on the youngest soils. Indeed, although some

352 studies suggest that P limitation increases phenol synthesis (Sampedro *et al.* 2011; Zhang *et al.*

353 2012) including along a long-term Hawaiian soil chronosequence (Hättenschwiller *et al.* 2003),

354 our results are in line with others showing that N limitation has a greater effect on quantitative plant

355 secondary metabolites (Koricheva *et al.* 1998; Wright *et al.* 2010; de Long *et al.* 2016).

356 The apparent stronger effect of N- compared with P limitation might be explained by their different

357 role in plant metabolism (Jones & Hartley 1999; Wright *et al.* 2010). Under N-limiting conditions,

358 there could be a surplus of photo-assimilates because leaf growth decreases sharply, while

359 photosynthesis continues, albeit at a somewhat slower rate (Prescott *et al.* 2020). The ammonium-

360 N in phenylalanine, which is a precursor of both aromatic amino acids and phenolic compounds,

361 would then be released and re-used in other N-containing molecules (Kováčik *et al.* 2007). The

362 rest of the phenylalanine molecule then becomes available for secondary metabolic pathways, in

363 which it is converted into C-based secondary metabolites such as phenylpropanoid derivatives

364 (Haukioja *et al.* 1998; Koricheva *et al.* 1998; Jones & Hartley 1999). This might explain why plants

365 growing on the young N limited environments had higher [phenols], eliminating a surplus of photo-

366 assimilates while conserving N. Under P-limiting conditions, however, any surplus of photo-

367 assimilates would be exported from the chloroplasts as P-containing compounds, and converted

368 into sucrose via reactions that release P, which is retained and reused (Stitt & Quick 1989).

369 Therefore, P-limiting conditions might not affect the pathway of secondary metabolite synthesis in

370 a way that N limitation does (Koricheva *et al.* 1998; Wright *et al.* 2010). Although the primary

371 function of plant phenolic compounds may be the release of N, rather than defense against

372 herbivores, it does make leaves less palatable for mammalian herbivores such as kangaroos

373   (Rafferty *et al.* 2005, 2010) on the youngest N-limited stages of the Jurien Bay chronosequence

374   (Fig. 5).

375   <mark>*Conclusions and Perspectives*</mark>

376   Leaf [phenols] and [Si] were negatively correlated when considering the means and CWM of each

377   community, all the individuals together, and within the Cyperaceae and Restionaceae family, which

378   suggest a tradeoff between both leaf defense strategies. This pattern was observed previously

379   (Cooke & Leishman 2012; Moles *et al.* 2013; Frew *et al.* 2016; Simpson *et al.* 2017; Waterman *et*

380   *al.* 2020), but never along a soil resource gradient. Here, the species growing on older soils and

381   adapted to nutrient-poor environments tend to favor silica accumulation over the synthesis of

382   phenols compared with species growing on younger soils.

383   Raven (1983) calculated that, on a weight basis, the energetic cost of incorporating 1 g of lignin is

384   about 27 times higher that of incorporating 1 g of SiO_2. Given the lower metabolic costs of

385   incorporating Si compared with others C-based compounds having similar functions (cellulose,

386   lignin, phenols) (Schoelynck *et al.* 2010; Cooke & Leishman 2012; Klotzbücher *et al.* 2018; de

387   Tombeur *et al.* 2020a), investing in silica as a defense mechanism (and eventually as leaf support

388   for Cyperaceae) would make sense from an energetic standpoint on the oldest and most nutrient-

389   depleted soils, where plants converge towards the 'slow' end of the leaf economics spectrum (Reich

390   2014; Guilherme Pereira *et al.* 2019). This energetic gain would save resources for other key

391   aspects of the plant life cycle like growth and reproduction during ecosystem retrogression, which

392   is key in these highly-infertile environments (Lambers 2014). Further studies should now

393   investigate other types of anti-herbivore defenses to better evaluate the overall investment in

394   defenses as a function of soil fertility along the Jurien Bay chronosequence. This is important given

395   that plants display a wide range of defense traits, without clear evidence of tradeoffs between them

396   globally (Moles *et al.* 2013). <mark>Overall, our study suggests that the type of nutrient limitation (i.e., N</mark>

397   <mark>vs P) may induce tradeoffs in plant defense strategies, opening up new perspectives about the role</mark>

398   <mark>of soil nutrient stoichiometry in the expression of plant defenses.</mark>

Acknowledgements

References

407   Aplin, T.E.. & Cannon, J.R. (1971). Distribution of alkaloids in some Western Australian plants.

408   *Econ. Bot.*, 25, 366–380.

409   Bettaieb Rebey, I., Bourgou, S., Ben Kaab, S., Aidi Wannes, W., Ksouri, R., Saidani Tounsi, M.,

410   *et al.* (2020). On the effect of initial drying techniques on essential oil composition, phenolic

411   compound and antioxidant properties of anise (*Pimpinella anisum* L.) seeds. *J. Food Meas.*

412   *Charact.*, 14, 220–228.

413   Bryant, J.P., Chapin, F.S. & Klein, D.R. (1983). Carbon/nutrient balance of boreal plants in

414   relation to vertebrate herbivory. *Oikos*, 40, 357–368.

415   Carey, J.C., Abbott, B.W. & Rocha, A. V. (2019). Plant Uptake Offsets Silica Release From a

416   Large Arctic Tundra Wildfire. *Earth's Futur.*, 7, 1044–1057.

417   Carey, J.C., Parker, T.C., Fetcher, N. & Tang, J. (2017). Biogenic silica accumulation varies

418   across tussock tundra plant functional type. *Funct. Ecol.*, 1–11.

419   Chao, T.T. & Sanzolone, R.F. (1992). Decomposition techniques. *J. Geochemical Explor.*, 44,

420   65–106.

421   Coley, P.D., Bryant, J.P. & Chapin, F.S. (1985). Resource availability and plant antiherbivore

422   defense. *Science (80-.).*, 230, 895–899.

423   Cooke, J. & Leishman, M.R. (2012). Tradeoffs between foliar silicon and carbon-based defences:

424   Evidence from vegetation communities of contrasting soil types. *Oikos*, 121, 2052–2060.

425   Cooke, J. & Leishman, M.R. (2016). Consistent alleviation of abiotic stress with silicon addition:

426   a meta-analysis. *Funct. Ecol.*, 30, 1340–1357.

427   Coskun, D., Deshmukh, R., Sonah, H., Menzies, J.G., Reynolds, O., Ma, J.F., *et al.* (2019). The

428   controversies of silicon's role in plant biology. *New Phytol.*, 221, 67–85.

429   Debona, D., Rodrigues, F.A. & Datnoff, L.E. (2017). Silicon's Role in Abiotic and Biotic Plant

430   Stresses. *Annu. Rev. Phytopathol.*, 55, 85–107.

431   Deshmukh, R., Sonah, H. & Belanger, R. (2020). New evidence defining the evolutionary path of

432   aquaporins regulating silicon uptake in land plants. *J. Exp. Bot.*

433   Deshmukh, R.K., Vivancos, J., Guérin, V., Sonah, H., Labbé, C., Belzile, F., *et al.* (2013).

434   Identification and functional characterization of silicon transporters in soybean using

435   comparative genomics of major intrinsic proteins in Arabidopsis and rice. *Plant Mol. Biol.*,

436   83, 303–315.

437   Endara, M.J. & Coley, P.D. (2011). The resource availability hypothesis revisited: A meta-

438   analysis. *Funct. Ecol.*, 25, 389–398.

439   Epstein, E. (1994). The anomaly of silicon in plant biology. *Proc. Natl. Acad. Sci. U. S. A.*, 91,

440   11–17.

441   Fauteux, F., Chain, F., Belzile, F., Menzies, J.G. & Bélanger, R.R. (2006). The protective role of

442   Si in the Arabidopsis-powdery mildew pathosystem. *Proc. Natl. Acad. Sci.*, 103, 17554–

443   17559.

444   Frew, A., Powell, J.R., Sallam, N., Allsopp, P.G. & Johnson, S.N. (2016). Trade-offs between

445   silicon and phenolic defenses may explain enhanced performance of root herbivores on

446   phenolic-rich plants. *J. Chem. Ecol.*, 42, 768–771.

447   Frew, A., Weston, L.A., Reynolds, O.L. & Gurr, G.M. (2018). The role of silicon in plant

448   biology: a paradigm shift in research approach. *Ann. Bot.*, 121, 1265–1273.

449   Garnier, E., Cortez, J., Billès, G., Navas, M.-L., Roumet, C., Debussche, M., *et al.* (2004). Plant

450   functional markers capture ecosystem properties during secondary succession. *Ecology*, 85,

451   2630–2637.

452   Garnier, E. & Navas, M.-L. (2013). Caractérisation fonctionnelle des végétaux. In: *Diversité*

453   *fonctionnelle des plantes* (ed. Boeck, D.). p. 353.

454   Guilherme Pereira, C., Hayes, P.E., O'Sullivan, O.S., Weerasinghe, L.K., Clode, P.L., Atkin,

455   O.K., *et al.* (2019). Trait convergence in photosynthetic nutrient-use efficiency along a 2-

456   million year dune chronosequence in a global biodiversity hotspot. *J. Ecol.*, 107, 2006–

457   2023.

458   Hall, A.D. & Morison, C.G.T. (1906). On the function of silica in the nutrition of cereals.—Part

459   I. *Proc. R. Soc. London. Ser. B*, 77, 455–477.

460   Hartley, S.E. & DeGabriel, J.L. (2016). The ecology of herbivore-induced silicon defences in

461   grasses. *Funct. Ecol.*, 30, 1311–1322.

462   Hättenschwiller, S., Hagerman, A.E. & Vitousek, P.M. (2003). Polyphenols in litter from tropical

463   montane forests across a wide range in soil fertility. *Biogeochemistry*, 64, 129–148.

464   Haukioja, E., Ossipov, V., Koricheva, J., Honkanen, T., Larsson, S. & Lempa, K. (1998).

465   Biosynthetic origin of carbon-based secondary compounds: Cause of variable responses of

466   woody plants to fertilization? *Chemoecology*, 8, 133–139.

467   Hayes, P., Turner, B.L., Lambers, H. & Laliberté, E. (2014). Foliar nutrient concentrations and

468   resorption efficiency in plants of contrasting nutrient-acquisition strategies along a 2-

469   million-year dune chronosequence. *J. Ecol.*, 102, 396–410.

470   Haymsom, M. & Chapman, L. (1975). Some aspects of the calcium silicate trials at Mackay.

471   *Proc. Queensl. Soc. Sugar Cane Technol.*, 42, 117–122.

472   Hodson, M.J., White, P.J., Mead, A. & Broadley, M.R. (2005). Phylogenetic variation in the

473   silicon composition of plants. *Ann. Bot.*, 96, 1027–1046.

474   Hothorn, T., Bretz, F. & Westfall, P. (2008). Simultaneous Inference in General Parametric

475   Models. *Biometrical J.*, 50, 346–363.

476   Ishizawa, H., Niiyama, K., Iida, Y., Shari, N.H.Z., Ripin, A. & Kitajima, K. (2019). Spatial

477   variations of soil silicon availability and biogenic silicon flux in a lowland tropical forest in

478   Malaysia. *Ecol. Res.*, 34, 548–559.

479   Johnson, S.N., Hartley, S.E., Ryalls, J.M.W., Frew, A. & Hall, C.R. (2020). Targeted plant

480   defense: silicon conserves hormonal defense signaling impacting chewing but not fluid-

481   feeding herbivores. *Ecology*, In press.

482   Johnson, S.N., Rowe, R.C. & Hall, C.R. (2019). Silicon is an inducible and effective herbivore

483   defence against *Helicoverpa punctigera* (Lepidoptera: Noctuidae) in soybean. *Bull.*

484   *Entomol. Res.*, 1–6.

485   Jones, C.G. & Hartley, S.E. (1999). A protein competition model of phenolic allocation. *Oikos*,

486   86, 27–44.

487   Katz, O. (2014). Beyond grasses: the potential benefits of studying silicon accumulation in non-

488   grass species. *Front. Plant Sci.*, 376, 1–3.

489   Kendrick, G.W., Wyrwoll, K.-H. & Szabo, B.J. (1991). Pliocene-Pleistocene coastal events and

490   history along the western margin of Australia. *Quat. Sci. Rev.*, 10, 419–439.

491   Klotzbücher, T., Klotzbücher, A., Kaiser, K., Vetterlein, D., Jahn, R. & Mikutta, R. (2018).

492   Variable silicon accumulation in plants affects terrestrial carbon cycling by controlling

493   lignin synthesis. *Glob. Chang. Biol.*, 24, 183–189.

494   Koricheva, J., Larsson, S., Haukioja, E. & Keinanen, M. (1998). Regulation of woody plant

495   secondary metabolism by resource availability: hypothesis testing by means of meta-

496   analysis. *Oikos*, 83, 212–226.

497   Kostic, L., Nikolic, N., Bosnic, D., Samardzic, J. & Nikolic, M. (2017). Silicon increases

498   phosphorus (P) uptake by wheat under low P acid soil conditions. *Plant Soil*, 419, 447–455.

499   Kováčik, J., Klejdus, B., Bačkor, M. & Repčák, M. (2007). Phenylalanine ammonia-lyase

500   activity and phenolic compounds accumulation in nitrogen-deficient *Matricaria chamomilla*

501   leaf rosettes. *Plant Sci.*, 172, 393–399.

502 Kraus, T.E.C., Zasoski, R.J. & Dahlgren, R.A. (2004). Fertility and pH effects on polyphenol and

503   condensed tannin concentrations in foliage and roots. *Plant Soil*, 262, 95–109.

504 Kumar, S., Soukup, M. & Elbaum, R. (2017). Silicification in Grasses: Variation between

505   Different Cell Types. *Front. Plant Sci.*, 8.

506 Laliberté, E., Turner, B.L., Costes, T., Pearse, S.J., Wyrwoll, K.H., Zemunik, G., *et al.* (2012).

507   Experimental assessment of nutrient limitation along a 2-million-year dune chronosequence

508   in the south-western Australia biodiversity hotspot. *J. Ecol.*, 100, 631–642.

509 Laliberté, E., Zemunik, G. & Turner, B.L. (2014). Environmental filtering explains variation in

510   plant diversity along resource gradients. *Science (80-.).*, 345, 1602–1605.

511 Lambers, H. (2014). *Plant Life on the Sandplains in Southwest Australia, a Global Biodiversity*

512   *Hotspot*. 2004th edn. Univerty of Western Australia Publishing, Crawley, Australia.

513 Lambers, H., Albornoz, F., Kotula, L., Laliberté, E., Ranathunge, K., Teste, F.P., *et al.* (2018).

514   How belowground interactions contribute to the coexistence of mycorrhizal and non-

515   mycorrhizal species in severely phosphorus-impoverished hyperdiverse ecosystems. *Plant*

516   *Soil*, 424, 11–33.

517 Lambers, H., Hayes, P.E., Laliberté, E., Oliveira, R.S. & Turner, B.L. (2015). Leaf manganese

518   accumulation and phosphorus-acquisition efficiency. *Trends Plant Sci.*, 20, 83–90.

519 Lambers, H. & Oliveira, R.S. (2019). *Plant Physiological Ecology, 3rd edition*. Springer

520   International Publishing.

521 Lambers, H. & Poorter, H. (1992). Inherent variation in growth rate between higher plants: a

522   search for physiological causes and ecological consequences. *Adv. Ecol. Res.*, 23, 187–261.

523   Lambers, H., Raven, J.A., Shaver, G.R. & Smith, S.E. (2008). Plant nutrient-acquisition

524   strategies change with soil age. *Trends Ecol. Evol.*, 23, 95–103.

525   Leroy, N., de Tombeur, F., Walgraffe, Y., Cornelis, J.-T. & Verheggen, F.J. (2019). Silicon and

526   Plant Natural Defenses against Insect Pests : Impact on Plant Volatile Organic Compounds

527   and Cascade E ff ects on Multitrophic Interactions. *Plants*, 8, 444.

528   de Long, J.R., Sundqvist, M.K., Gundale, M.J., Giesler, R. & Wardle, D.A. (2016). Effects of

529   elevation and nitrogen and phosphorus fertilization on plant defence compounds in subarctic

530   tundra heath vegetation. *Funct. Ecol.*, 30, 314–325.

531   Ma, J.F. & Takahashi, E. (1990). Effect of silicon on the growth and phosphorus uptake of rice.

532   *Plant Soil*, 126, 115–119.

533   Ma, J.F., Tamai, K., Yamaji, N., Mitani, N., Konishi, S., Katsuhara, M., *et al.* (2006). A silicon

534   transporter in rice. *Nature*, 440, 688–691.

535   Massey, F. & Hartley, S. (2009). Physical defences wear you down : progressive and irreversible

536   impacts of silica on insect herbivores. *J. Anim. Ecol.*, 78, 281–291.

537   Massey, F.P., Ennos, A.R. & Hartley, S.E. (2006). Silica in grasses as a defence against insect

538   herbivores: Contrasting effects on folivores and a phloem feeder. *J. Anim. Ecol.*, 75, 595–

539   603.

540   Massey, F.P., Ennos, A.R. & Hartley, S.E. (2007). Grasses and the resource availability

541   hypothesis: The importance of silica-based defences. *J. Ecol.*, 95, 414–424.

542   Massey, F.P. & Hartley, S.E. (2006). Experimental demonstration of the antiherbivore effects of

543   silica in grasses: impacts on foliage digestibility and vole growth rates. *Proc. R. Soc. B Biol.*

544   *Sci.*, 273, 2299–2304.

545   McArthur, W.M. & Bettenay, E. (1974). *Development and distribution of soils of the Swan*

546   *Coastal Plain, Western Australia. Canberra: CSIRO*. CSIRO. Melbourne.

547   McNaughton, S.J., Tarrants, J.L., McNaughton, M.M. & Davis, R.D. (1985). Silica as a defense

548   against herbivory and a growth promotor in african grasses. *Ecology*, 66, 528–535.

549   Moles, A.T., Peco, B., Wallis, I.R., Foley, W.J., Poore, A.G.B., Seabloom, E.W., *et al.* (2013).

550   Correlations between physical and chemical defences in plants: Tradeoffs, syndromes, or

551   just many different ways to skin a herbivorous cat? *New Phytol.*, 198, 252–263.

552   Motomura, H., Mita, N. & Suzuki, M. (2002). Silica accumulation in long-lived leaves of *Sasa*

553   *veitchii* (Carrière) rehder (Poaceae-Bambusoideae). *Ann. Bot.*, 90, 149–152.

554   Nakamura, R., Ishizawa, H., Wagai, R., Suzuki, S., Kitayama, K. & Kitajima, K. (2019). Silicon

555   cycled by tropical forest trees: effects of species, elevation and parent material on Mount

556   Kinabalu, Malaysia. *Plant Soil*, 443, 155–166.

557   Neu, S., Schaller, J. & Dudel, E.G. (2017). Silicon availability modifies nutrient use efficiency

558   and content, C:N:P stoichiometry, and productivity of winter wheat (*Triticum aestivum* L.).

559   *Sci. Rep.*, 7, 40829.

560   Northup, R.R., Yu, Z., Dahlgren, R.A. & Vogt, A. (1995). Polyphenol control of nitrogen release

561   from pine litter. *Nature*, 377, 227–229.

562   Pang, J., Bansal, R., Zhao, H., Bohuon, E., Lambers, H., Ryan, M.H., *et al.* (2018). The

563   carboxylate-releasing phosphorus-mobilizing strategy can be proxied by foliar manganese

564   concentration in a large set of chickpea germplasm under low phosphorus supply. *New*

565   *Phytol.*, 219, 518–529.

566   Peltzer, D.A., Wardle, D.A., Allison, V.J., Baisden, W.T., Bardgett, D., Chadwick, O.A., *et al.*

567   (2010). Understanding ecosystem retrogression. *Ecol. Monogr.*, 80, 509–529.

568   Pinheiro, J., Bates, D., DebRoy, S., Sarkar, D. & Team, R.C. (2020). nlme: Linear and Nonlinear

569   Mixed Effects Models.

570   Playford, P.E., Cockbain, A.E. & Lowe, G.H. (1976). *Geology of the Perth Basin, Western*

571   *Australia*. Perth, W.A.

572   Prescott, C.E., Grayston, S.J., Helmisaari, H., Ka, E., Körner, C., Lambers, H., *et al.* (2020).

573   Surplus Carbon Drives Allocation and Plant – Soil Interactions, xx, 1–9.

574   Putra, R., Powell, J.R., Hartley, S.E. & Johnson, S.N. (2020). Is it time to include legumes in

575   plant silicon research? *Funct. Ecol.*, 34, 1142–1157.

576   Quigley, K.M., Griffith, D.M., Donati, G.L. & Anderson, T.M. (2020). Soil nutrients and

577   precipitation are major drivers of global patterns of grass leaf silicification. *Ecology*, 101, 1–

578   10.

579   Rafferty, C., Lamont, B.B. & Hanley, M.E. (2005). Selective feeding by kangaroos (Macropus

580   fuliginosus) on seedlings of Hakea species: Effects of chemical and physical defences. *Plant*

581   *Ecol.*, 177, 201–208.

582   Rafferty, C.M., Lamont, B.B. & Hanley, M.E. (2010). Herbivore feeding preferences in captive

583   and wild populations. *Austral Ecol.*, 35, 257–263.

584   Raven, J.A. (1983). The transport and function of silicon in plants. *Biol. Rev.*, 58, 179–207.

585   Reich, P.B. (2014). The world-wide "fast-slow" plant economics spectrum: A traits manifesto. *J.*

Ecol., 102, 275–301.

586

587   Salminen, J.P. & Karonen, M. (2011). Chemical ecology of tannins and other phenolics: We need

588   a change in approach. *Funct. Ecol.*, 25, 325–338.

589   Sampedro, L., Moreira, X. & Zas, R. (2011). Costs of constitutive and herbivore-induced

590   chemical defences in pine trees emerge only under low nutrient availability. *J. Ecol.*, 99,

591   818–827.

592   Sauer, D., Saccone, L., Conley, D.J., Herrmann, L. & Sommer, M. (2006). Review of

593   methodologies for extracting plant-available and amorphous Si from soils and aquatic

594   sediments. *Biogeochemistry*, 80, 89–108.

595   Schaller, J., Brackhage, C. & Dudel, E.G. (2012). Silicon availability changes structural carbon

596   ratio and phenol content of grasses. *Environ. Exp. Bot.*, 77, 283–287.

597   Schaller, J., Turner, B.L., Weissflog, A., Pino, D., Bielnicka, A.W. & Engelbrecht, B.M.J.

598   (2018). Silicon in tropical forests: large variation across soils and leaves suggests ecological

599   significance. *Biogeochemistry*, 140, 161–174.

600   Schoelynck, J., Bal, K., Backx, H., Okruszko, T., Meire, P. & Struyf, E. (2010). Silica uptake in

601   aquatic and wetland macrophytes: A strategic choice between silica, lignin and cellulose?

602   *New Phytol.*, 186, 385–391.

603   Simpson, K.J., Wade, R.N., Rees, M., Osborne, C.P. & Hartley, S.E. (2017). Still armed after

604   domestication? Impacts of domestication and agronomic selection on silicon defences in

605   cereals. *Funct. Ecol.*, 31, 2108–2117.

606   Stitt, M. & Quick, W.P. (1989). Photosynthetic carbon partitioning: its regulation and

1
2
3
4
5
6
7
8
9
10
11
12
13
14
15
16
17
18
19
20
21
22
23
24
25
26
27
28
29
30
31
32
33
34
35
36
37
38
39
40
41
42
43
44
45
46
47
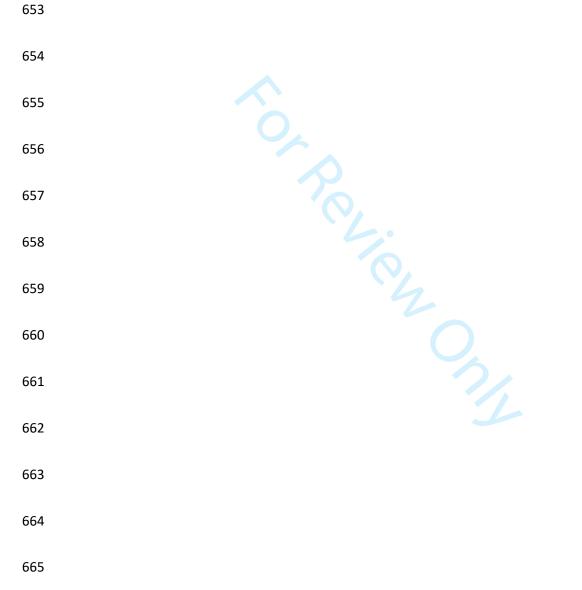48
49
50
51
52
53
54
55
56
57
58
59
60

607   possibilities for manipulation. *Physiol. Plant.*, 77, 633–641.

608   Teodoro, G.S., Lambers, H., Nascimento, D.L., de Britto Costa, P., Flores-Borges, D.N.A.,

609   Abrahão, A., *et al.* (2019). Specialized roots of Velloziaceae weather quartzite rock while

610   mobilizing phosphorus using carboxylates. *Funct. Ecol.*, 33, 762–773.

611   de Tombeur, F., Vander Linden, C., Cornélis, J.-T., Godin, B., Compère, P. & Delvaux, B.

612   (2020a). Soil and climate affect foliar silicification patterns and silica-cellulose balance in

613   sugarcane (*Saccharum officinarum*). *Plant Soil*, 452, 529–546.

614   de Tombeur, F., Turner, B.L., Laliberté, E., Lambers, H. & Cornelis, J.T. (2020b). Silicon

615   Dynamics During 2 Million Years of Soil Development in a Coastal Dune Chronosequence

616   Under a Mediterranean Climate. *Ecosystems*, 23, 1614–1630.

617   de Tombeur, F., Turner, B.L., Laliberté, E., Lambers, H., Mahy, G., Faucon, M.P., *et al.* (2020c).

618   Plants sustain the terrestrial silicon cycle during ecosystem retrogression. *Science (80-.).*,

619   369, 1245–1248.

620   Trembath-Reichert, E., Wilson, J.P., McGlynn, S.E. & Fischer, W.W. (2015). Four hundred

621   million years of silica biomineralization in land plants. *Proc. Natl. Acad. Sci. U. S. A.*, 112,

622   5449–54.

623   Turner, B.L., Hayes, P.E. & Laliberté, E. (2018). A climosequence of chronosequences in

624   southwestern Australia. *Eur. J. Soil Sci.*, 69, 69–85.

625   Turner, B.L. & Laliberté, E. (2015). Soil development and nutrient availability along a 2 million-

626   year coastal dune chronosequence under species-rich mediterranean shrubland in

627   Southwestern Australia. *Ecosystems*, 18, 287–309.

628   Violle, C., Navas, M.L., Vile, D., Kazakou, E., Fortunel, C., Hummel, I., *et al.* (2007). Let the

629   concept of trait be functional! *Oikos*, 116, 882–892.

630   Vitousek, P. (2004). *Nutrient Cycling and Limitation - Hawai'i as Model System*. Princeton

631   University Press, New Jersey.

632   Vitousek, P.M., Walker, L.R., Whiteaker, L.D. & Matson, P.A. (1993). Nutrient limitations to

633   plant growth during primary succession in Hawaii Volcanoes National Park.

634   *Biogeochemistry*, 23, 197–215.

635   Waterman, J.M., Hall, C.R., Mikhael, M., Cazzonelli, C.I., Hartley, S.E. & Johnson, S.N. (2020).

636   Short-term resistance that persists: Rapidly induced silicon anti-herbivore defence affects

637   carbon-based plant defences. *Funct. Ecol.*

638   Wright, D.M., Jordan, G.J., Lee, W.G., Duncan, R.P., Forsyth, D.M. & Coomes, D.A. (2010). Do

639   leaves of plants on phosphorus-impoverished soils contain high concentrations of phenolic

640   defence compounds? *Funct. Ecol.*, 24, 52–61.

641   Wright, I.J., Westoby, M., Reich, P.B., Oleksyn, J., Ackerly, D.D., Baruch, Z., *et al.* (2004). The

642   worldwide leaf economics spectrum. *Nature*, 428, 821–827.

643   Zemunik, G., Turner, B.L., Lambers, H. & Laliberté, E. (2015). Diversity of plant nutrient-

644   acquisition strategies increases during long-term ecosystem development. *Nat. Plants*, 1, 1–

645   4.

646   Zemunik, G., Turner, B.L., Lambers, H. & Laliberté, E. (2016). Increasing plant species diversity

647   and extreme species turnover accompany declining soil fertility along a long-term

648   chronosequence in a biodiversity hotspot. *J. Ecol.*, 104, 792–805.

649 Zhang, L.H., Shao, H.B., Ye, G.F. & Lin, Y.M. (2012). Effects of fertilization and drought stress

650 on tannin biosynthesis of *Casuarina equisetifolia* seedlings branchlets. *Acta Physiol. Plant.*,

651 34, 1639–1649.

652

653

654

655

656

657

658

659

660

661

662

663

664

665

666

667

Figures Captions

Fig. 1 – Leaf silicon (Si) concentrations across the chronosequence stages considering all individuals (i) and the means (ii) and cover-weighted means (CWM) (iii) of the five plots per stage (a). Leaf total phenol concentrations for the same chronosequence stages and plots (b). In the box-plots, small black dots represent each individual and large black dots represent outliers (outside 1.5*inter-quartile range). In the second and third panels, black dots indicate means and bars show 95% confidence intervals (n=5). In (a), Fisher LSD groupings (p<0.05) were performed on log-transformed data for the first plot and on root-square-transformed data for the two others, as the scales of the axes.

Fig. 2 – Soil total phosphorus (P) concentrations, total nitrogen (N) concentrations and soil N to P ratio versus cover-weighted mean (CWM) leaf silicon (Si) concentrations (a) and CWM leaf total phenol concentrations (b) (n = 25 plots). Black lines indicate the regression lines between both variables, shaded areas represent 95% confidence interval of the regression and colors of the circles indicate the chronosequence stages. Axes were log-transformed for soil total P concentration and N to P ratio and root-square-transformed for CWM leaf Si concentration. The p-values of the corresponding linear mixed-effect models are indicated if < 0.05. Regression lines were removed if the model p-values were > 0.05.

Fig. 3 – Leaf total phenol concentrations versus leaf silicon (Si) concentrations considering all individuals (a) and the means (b) and cover-weighted means (CWM) (c) of the five plots per stage. Scatterplot correlation matrix of leaf concentrations of Si, total phenols (Phnl), potassium (K), calcium (Ca), magnesium (Mg) and phosphorus (P) considering all individuals, the means, and CWM of the five plots per stage (d). In (a), (b) and (c), black lines indicate the regression lines between both variables, shaded areas represent 95% confidence interval of the regression and

691   colors of the circles indicate the chronosequence stages. Y-axes were log-transformed in (a) and

692   root-square-transformed in (b) and (c). The p-values of the corresponding linear mixed-effect

693   models are indicated if < 0.05. In (d), the size and color of the squares represent Pearson's

694   correlation coefficient. All correlations having a p-value > 0.01 are represented by a blank space.

695   Plots on the diagonal represent the distributions of each variable. Concentrations are in gram per

696   kg dry weight for the nutrients and gallic acid equivalent (GAE) gram per kg dry weight for total

697   phenols. In (d), axes were log-transformed for all variables, except for leaf [phenols] in the first

698   plot, while root-square-transformed for leaf [Si], [Ca] and [K] and log-transformed for leaf [P] and

699   [Mg] in the second and third plots.

700   **Fig. 4 –** Leaf silicon (Si) (a) and total phenol concentrations (b) across the chronosequence stages

701   for Cyperaceae, and relationship between both for the same individuals (c). In (a) and (b), the small

702   black dots represent each species and large black dots represent outliers (outside 1.5*inter-quartile

703   range). In (a), Fisher LSD groupings (p<0.05) were performed on root-square-transformed data, as

704   the scale of the axes. In (c), the y-axis was root-square-transformed; each symbol represents a

705   different species, the black line indicates the regression line between both variables, the shaded

706   area represents 95% confidence interval of the regression, and the p-value of the corresponding

707   linear mixed-effect model is indicated.

708   **Fig. 5 –** Schematic representation (adapted from Lambers *et al.* 2008) of changes in soil total

709   phosphorus (P) and nitrogen (N), P-acquisition strategies, and leaf defense strategies during long-

710   term ecosystem development. Changes in soil P and N are based on Hayes *et al.* (2014). At the

711   Jurien Bay chronosequence, soil total P concentration continually declines with increasing soil age,

712   from about 430 to 6 mg kg^{-1}, while total N concentration increases from 0.5 to 1.2 g kg^{-1} in the

713   young soils where total [P] is relatively high, then declines to 0.2 g kg^{-1} in the oldest soil, resulting

714　in a shift from N to P limitation of plant growth. The changes in nutrient-acquisition strategies were

715　originally suggested by Lambers *et al.* (2008), but subsequently confirmed in Zemunik *et al.*

716　(2015). Along the Jurien Bay chronosequence, the relative cover declines for arbuscular

717　mycorrhizal and ectomycorrhizal species, but increases for carboxylate-releasing cluster-rooted

718　species and others with functionally equivalent strategies. The changes in silica and phenol-based

719　defenses are based on the present study.

720 **Tables**

721 **Table 1** – Main properties of the five chronosequence stages used in this study. The chronosequence stages, dune system, geological

722 formation and estimated soil age are based on Laliberté *et al.* (2012) and Turner & Laliberté (2015). The carbonate, total phosphorus (P)

723 and nitrogen (N) concentrations, soil total N to total P ratio, pH-CaCl$_2$ and cation exchange capacity (CEC) are based on Hayes *et al.*

724 (2014) and Zemunik *et al.* (2016). They result from seven soil samples (0-20 cm deep) taken in each of the five plots by chronosequence

725 stage used in this study (n = 25 plots). The limiting nutrients are based on Laliberté *et al.* (2012) and Hayes *et al.* (2014). The expected

726 silicon (Si) availability are from de Tombeur *et al.* (2020b, c).

Stage	Dune system	Geological formation	Estimated soil age (ka)	Carbonates[*] (%)	pH-CaCl$_2$[†]	CEC[†] (cmolc kg^{-1})	Total P[†] (mg kg^{-1})	Total N[†] (g kg^{-1})	Soil total N to total P ratio[†]	Limiting nutrients	Expected Si availability
1	Quindalup young	Safety Bay Sand	0.1 (Holocene)	75.2(3.5)	8.2(0.1)	30.5(4.5)	351.0(6.6)	0.5(0.0)	1.4(0.1)	N	Very low
2	Quindalup medium	Safety Bay Sand	1 (Holocene)	75.5(2.8)	7.8(0.0)	12.2(1.1)	424.4(8.3)	1.2(0.0)	2.7(0.4)	N, P and/or other nutrients	Very low
3	Quindalup old	Safety Bay Sand	6.7 (Holocene)	25.6(3.7)	7.8(0.0)	10.9(0.5)	205.7(7.0)	0.7(0.0)	3.6(0.5)	N, P and/or other nutrients	Low
4	Spearwood	Tamala Limestone	125 (Middle Pleistocene)	BDL	5.8(0.1)	3.6(0.2)	18.5(1.0)	0.2(0.0)	10.7(1.9)	P	Medium
5	Bassendean	Bassendean sand	>2000 (Early Pleistocene or Late Pliocene)	BDL	4.8(0.1)	2.5(0.2)	6.6(0.5)	0.2(0.0)	30.8(8.5)	P	Low

727 [*]SE is indicated in brackets. The seven soil samples were bulked before analysis (n=5).
728 [†]SE is indicated in brackets (n=35).
729 BDL, below detections limits

Concentrations in g kg⁻¹ DW for the nutrients (transformations in the legend) and GAE g kg⁻¹ DW for the phenols

(a) Cyperaceae — Leaf Si (g kg⁻¹) vs Chronosequence stage

(b) Cyperaceae — Leaf phenols (GAE g kg⁻¹) vs Chronosequence stage

(c) Cyperaceae — Leaf Si (g kg⁻¹) vs Leaf phenols (GAE g kg⁻¹), p=0.0158

Legend: Ficinia nodosa, Gahnia sp. South West, Lepidosperma calcicola, Lepidosperma costale, Mesomelaena pseudostygia, Schoenus brevisetis, Schoenus curvifolius, Schoenus grandiflorus, Schoenus pedicellatus